J. Inv. Ill-Posed Problems **15** (2007), 12–39 DOI 10.1515 / JIP.2007.002

Iterative Multilevel Algorithm Using Modified Landweber Iterations With Application to Piezoelectricity

Tom Lahmer

Communicated by Name of Editor

Abstract. In piezoelectric applications, especially when the devices are used as actuators, the piezoelectric materials are driven under large signals which cause a nonlinear behavior. Our aim is to model the nonlinearities by functional dependencies of the material parameters on the electric field strength. The focus lies in the inverse problem, namely the identification of the parameter curves by appropriate measuremets of charge signals over time. Since the measured data are contaminated with data noise we deal with a typically *ill-posed* problem. The solution requires regularizing methods where we consider modified Landweber iterations, namely the *steepest descent* and *minimal error method* together with *a posteriori* stopping rules. Since any implementation requires a discretization of the parameter curves an iterative multilevel algorithm is proposed where the iterations begin with coarse discretizations of the sought-for quantities profiting from the inherent regularization property of coarse discretization. At an advanced state of the iterations the algorithm switches to finer levels of discretization. By this a sufficiently smooth resolution of the sought-for quantities can be achieved. Convergence results and the regularizing property of such an iterative multilevel algorithm using modified Landweber iterations on each level will be proven. The application to the above mentioned inverse problem in piezoelectricity together with numerical results closes this article.

Key words. Parameter identification, regularization, multilevel, modified Landweber, steepest descent, minimal error, piezoelectricity.

AMS classification. 65J15, 65J20, 65J22, 65M32, 65Z05.

Supported by the German Science Foundation DFG under grant Ka 1778/1

1. Introduction

Piezoelectric transducers convert electrical signals into mechanical ones and vice versa.

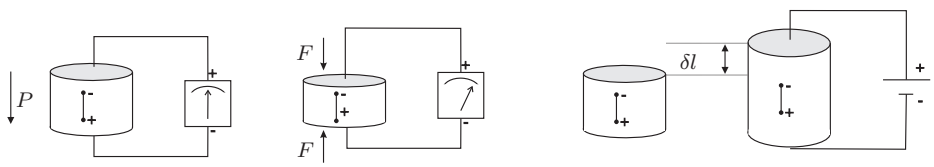

Figure 1: Piezoelectric effect. Left pictures: Direct piezoelectric effect, i.e. the generation of an electrical signal by a mechanical force. Right pictures: Converse piezoelectric effect, i.e. shape deformation due to an applied voltage or charge.

So, the term piezoelectricity is endowed with two effects: The direct effect on one hand, i.e. the conversion of a mechanical force into an electric signal which is typical for sensor applications (e.g. force and acceleration sensors). On the other hand there is the indirect or inverse piezoelectric effect, i.e. the mechanical excitation by application of an electric field (actuator applications, e.g. ultrasound generation, stack actuators) [1].

The paper is organized as follows. After a brief derivation of the piezoelectric constitutive equations and partial differential equations with the unknown quantities mechanical displacement and electric potential, we show how nonlinearities can be modeled for moderate electric fields. Then we turn to the theoretical investigation of an iterative multilevel algorithm, which is strongly motivated by the work of Scherzer [21]. Here, modified Landweber iterations are considered as inner iterations on each level, which allow for an appropriate choice of the relaxation parameter in the Landweber iteration improving the speed of convergence without increasing the computational costs. Convergence results and the regularization property of the iterative multilevel algorithm are in the focus. This article closes with the application of the derived algorithm to the simulation based (FEM) identification of material parameter curves in nonlinear piezoelectricity.

1.1. Material Laws and Partial Differential Equations

The piezoelectric effect in the linear case is described by the following constitutive equations [6],

$$\begin{aligned} \vec{\sigma} &= \mathbf{c}^E \vec{S} - \mathbf{e}^T \vec{E} \\ \vec{D} &= \mathbf{e}\vec{S} + \boldsymbol{\varepsilon}^S \vec{E}, \end{aligned} \tag{1.1}$$

where $\vec{\sigma}$ is the mechanical stress tensor and $\vec{D}$ the dielectric displacement. Further (1.1) involves the mechanical strain $\vec{S}$ and the electric field $\vec{E}$, respectively. The material tensors are the fourth order modulus of elasticity $\mathbf{c}^E$ $(\mathrm{N/m^2})$ at constant electric field, the third order piezoelectric coupling $\mathbf{e}$ $(\mathrm{N/Vm})$, and the second order permittivity tensor $\boldsymbol{\varepsilon}^S$ $(\mathrm{C/Vm})$ at constant strain. The symmetry and the sparsity of the material tensors involved can be seen in (3.5) by assuming all entries to be constants. We additionally refer to [1, 6, 8, 10].

Together with Newton's law of motion the fact that piezoelectric materials are insulators we obtain

$$\begin{aligned} \rho \frac{\partial^2 \mathbf{u}}{\partial t^2} - \mathbf{B}^T \Big(\mathbf{c}^E \mathbf{B}\mathbf{u} + \mathbf{e}^T \nabla \phi \Big) &= 0 \quad \text{in } \Omega \\ \nabla \cdot \Big(\mathbf{e}\mathbf{B}\mathbf{u} - \boldsymbol{\varepsilon}^S \nabla \phi \Big) &= 0 \quad \text{in } \Omega\,, \end{aligned} \tag{1.2}$$

where by Faraday's law, the electric field is the negative gradient of the electric potential ϕ [5]

$$\vec{E} = -\nabla \phi \tag{1.3}$$

with $\nabla := (\frac{\partial}{\partial x}, \frac{\partial}{\partial y}, \frac{\partial}{\partial z})$. By linearized elasticity the strain is the spatial variation of the mechanical displacement $\mathbf{u}$

$$\vec{S} = \mathbf{B}\mathbf{u}. \tag{1.4}$$

The three dimensional differential operator relates mechanical strains to the mechanical displacements

$$\mathbf{B} := \begin{pmatrix} \frac{\partial}{\partial x} & . & . & . & \frac{\partial}{\partial z} & \frac{\partial}{\partial y} \\ . & \frac{\partial}{\partial y} & . & \frac{\partial}{\partial z} & . & \frac{\partial}{\partial x} \\ . & . & \frac{\partial}{\partial z} & \frac{\partial}{\partial y} & \frac{\partial}{\partial x} & . \end{pmatrix}^T . \tag{1.5}$$

As boundary conditions we consider the experimental setting of vanishing normal

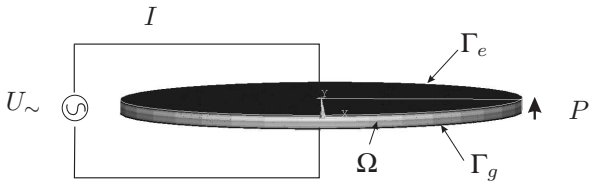

Figure 2: Piezoelectric disc. Notation of boundaries. This shape is for example used to simulate radial or thickness modes. The direction of polarization is marked with P.

stresses at the boundary $\partial\Omega$. Two electrodes are applied at opposite surfaces Γ_g and Γ_e of Ω, see Figure 2. One of them is loaded with a prescribed potential ϕ^e, the other one is grounded. Further, on the parts of the boundary which are not covered by any electrode there shall be no free charge. Together, this gives the following boundary conditions

$$\begin{aligned} \mathbf{N}^T\vec{\sigma} &= 0 \quad \text{on } \partial\Omega \\ \phi &= 0 \quad \text{on } \Gamma_g \\ \phi &= \phi^e \quad \text{on } \Gamma_e \\ \vec{D}\cdot\vec{n} &= 0 \quad \text{on } \Gamma_R := \partial\Omega \setminus (\Gamma_e \cup \Gamma_g), \end{aligned} \tag{1.6}$$

where

$$\mathbf{N} = \begin{pmatrix} n_x & . & . & . & n_z & n_y \\ . & n_y & . & n_z & . & n_x \\ . & . & n_z & n_y & n_x & . \end{pmatrix}^T$$

and $\vec{n} = (n_x, n_y, n_z)$ is the outer unit normal vector. Additionally, appropriate initial conditions are given by

$$\begin{aligned} \mathbf{u}(\cdot, 0) &= \mathbf{u}_0 \\ \dot{\mathbf{u}}(\cdot, 0) &= \mathbf{u}_1. \end{aligned} \tag{1.7}$$

Concerning the electric field strengths one can assume linear behavior only in the range of $0.0 - 0.1\mathrm{kV/mm}$. Above these field strengths nonlinear effects occur. Signals with which piezoelectric actuators are usually driven cause fields of $0.2 - 0.3\mathrm{kV/mm}$, thus the actuators mainly operate in nonlinear ranges [4]. In order to model the nonlinear behavior we consider higher order terms in the constitutives, which can be seen as a special case of functional dependencies of the material tensors on the field quantities strain and electric field. The model allows to describe nonlinear effects for moderate electric fields staying below the coercive field strength. Effects like a nonlinear relation between applied voltage and displacement, jump phenomena in the response spectra, appearance of higher harmonics, and softening of the material are already visible at weak fields [18, 19]. In our model the nonlinear effects are assumed to be reversible, i.e. no depolarization of the crystals in the piezoelectric material is expected as opposed to models regarding hysteresis [11, 23]. The constitutives in their most general form considering material nonlinearities read as [12]

$$\vec{\sigma} = \mathbf{c}^E(\vec{S})\vec{S} - \mathbf{e}^T(\vec{S},\vec{E})\vec{E} \tag{1.8}$$

$$\vec{D} = \mathbf{e}(\vec{E},\vec{S})\vec{S} + \boldsymbol{\varepsilon}^S(\vec{E})\vec{E}. \tag{1.9}$$

The now nonlinear set of differential equations in (1.2) is solved with the Finite Element Method using the Newmark scheme for time integration and a damped fixed-point iteration to solve the nonlinear problem at each time-step. For details we refer to [10, 14].

The inverse problem of parameter identification formulated with a parameter-to-solution mapping F corresponds to the problem of solving a nonlinear operator equation.

2. Iterative Multilevel Algorithm

The mathematical problem which we have in mind is the following

$$\begin{aligned} F : D(F) &\rightarrow Y \quad \text{with} \quad D(F) \subseteq X \\ F(p) &= y^\delta, \end{aligned} \tag{2.1}$$

where F is a nonlinear operator mapping from the infinite dimensional Hilbert space X into Y. The value p is the sought-for quantity and y^δ is the noisy input, in general measurements of physical quantities with

$$||y - y^\delta|| < \delta \tag{2.2}$$

where δ is a measure for the noise level and y denotes noisefree data.

Motivated by the efficiency of a multilevel strategy on one hand and by the speed up of convergence of minimal error and steepest descent method as compared to classical Landweber, on the other hand we aim at carrying over the results by Scherzer [21] on multilevel Landweber to modified versions of Landweber's iteration, namely the

steepest descent and minimal error method [9]. Let us introduce the general assumptions considered in the sequel. The operator F in (2.1) is assumed to be continuous, differentiable and its Frechét derivative F' to be Lipschitz continuous and normalized such that

$$||F'(p)|| \leq 1, \ \ \forall\, p \ \in D(F). \tag{2.3}$$

Further, we assume that $\mathcal{N}(F'(p))$ is trivial for all $p \in \mathcal{B}_\rho(p^0)$.
The numerical realization of the modified Landweber iterations is now considered in a finite dimensional subspace $X_N := P_N X$ of X, where P_N denotes the orthogonal projection onto

$$X_N \subseteq X, \quad \text{with} \quad X_0 \subseteq X_1 \subseteq ... \subseteq X_N \quad \text{and} \quad \overline{\bigcup_{N\in\mathbb{N}} X_N} = X. \tag{2.4}$$

Let the union $\cup_{N\in\mathbb{N}} X_N$ be dense in X. The initial guess at discretization level N is denoted by p_N^0.
Moreover the tangential cone condition is assumed to hold on the discrete subspaces X_N

$$\begin{aligned} ||F(p) - F(P_N p^\dagger) - F'(p)(p - P_N p^\dagger)|| &\leq \eta_N ||F(p) - F(P_N p^\dagger)|| \\ \text{for all } p \in X_N \cap \mathbf{B}_{\rho/2}(P_N p^\dagger) \subseteq D(F) &\text{ with } \eta_N \leq \frac{1}{4}. \end{aligned} \tag{2.5}$$

At each level, the modified Landweber iteration now reads as follows,

$$p_N^{k+1,\delta} = p_N^{k,\delta} + \omega_N^{k,\delta} s_N^{k,\delta}, \qquad s_N^{k,\delta} := P_N F'(p_N^{k,\delta})^*(y^\delta - F(p_N^{k,\delta})) \tag{2.6}$$

where the coefficients $\omega_N^{k,\delta}$ are chosen either as

$$\omega_N^{k,\delta} := \frac{||s_N^{k,\delta}||^2}{||F'(p_N^{k,\delta}) s_N^{k,\delta}||^2} \tag{2.7}$$

or as

$$\omega_N^{k,\delta} := \frac{||y^\delta - F(p_N^{k,\delta})||^2}{||s_N^{k,\delta}||^2}. \tag{2.8}$$

These choices transform the classical Landweber iteration into a discrete version of the steepest descend or minimal error method, respectively. See [9, 16, 20] for the infinite dimensional case of these methods. By (2.3) for both choices

$$\omega_N^{k,\delta} \geq 1 \tag{2.9}$$

holds.
The size of the discretization parameter N is rather crucial. A small value of N does not allow for a precise approximation. However the iteration might be very sensitive to noise in the data when using a large N. Further, depending on the implementation a large N makes the iterations extremely time consuming, e.g. if one thinks of approximating F' by finite differences.

Concerning the stopping criteria in each level the residual is tested by a combination of an approximation estimate for the current level and the data error level. The approximation error may be estimated either in X or Y which gives the following two criteria

$$||F(p_N^{k+1,\delta}) - y^\delta|| \leq C_1(\delta + ||F(P_N p^\dagger) - F(p^\dagger)||) \tag{2.10}$$

or

$$||F(p_N^{k+1,\delta}) - y^\delta|| \leq \tilde{C}_1(\delta + ||(P_N - I)p^\dagger||). \tag{2.11}$$

Each of them determines a well-defined stopping index $\overline{k}_*(N,\delta)$ at level N , i.e.

$$\overline{k}_*(N,\delta) := \min\{k \in \mathbb{N} \mid \text{where (2.10) holds}\} \tag{2.12}$$

and analogously for (2.11). In the sequel we assume $C_1 = \tilde{C}_1$.

The stopping rules (2.10) and (2.11) are used for theoretical purposes; in a practical implementation the terms $||F(P_N p^\dagger) - F(p^\dagger)||$ and $||(P_N - I)p^\dagger||$ containing the unknown solution have to be estimated based on *a priori* information on $p^\dagger$, see for example [13, 15, 21, 22]. Obviously, as long as the iterations are not terminated we have for all $k < \overline{k}_*(N,\delta)$

$$||F(p_N^{k,\delta}) - y^\delta|| \quad > \quad C_1(\delta + ||F(P_N p^\dagger) - y||), \tag{2.13}$$

or

$$||F(p_N^{k,\delta}) - y^\delta|| \quad > \quad C_1(\delta + ||(P_N - I)p^\dagger||). \tag{2.14}$$

Note that the stopping criterion might get active at $k = 0$ so that there is no k satisfying (2.14) (or (2.13)). It is a crucial assumption in [21] and also in some (but not all) assertions made here, that at least one step is carried out on level N, i.e. (2.14) (or (2.13)) is satisfied for $k = 0$.

Even though the choice of $\overline{k}_*(N,\delta)$ in (2.12) avoids an undesired amplification of the data error, the stopping criterion has a minor drawback since it does not guarantee that the number of iterations is finite in each level. This however is necessary in order to compute the initial guess at any subsequent level. As a consequence we introduce some *a priori* chosen finite maximal number $\tilde{k}_{\max}(N)$ of iterations

$$0 < \tilde{k}_{\max}(N) < \infty. \tag{2.15}$$

A combination of (2.12) and (2.15), i.e.

$$k_*(N,\delta) := \min\{\overline{k}_*(N,\delta), \tilde{k}_{\max}(N)\} < \infty \tag{2.16}$$

gives a well suited, finite stopping index for the inner iterations of the multilevel algorithm.

Refinement of the discretization, i.e. the outer iteration will be performed until an *a posteriori* stopping rule becomes active

$$||y^\delta - F(p_N^{k_*,\delta})|| \leq C_2\delta \leq ||y^\delta - F(p_N^{k,\delta})||, \quad C_2 > 2\frac{1+\eta_N}{1-2\eta_N} > 2. \tag{2.17}$$

Only as long as this global discrepancy principle does not terminate the iterations one continues at the next level $N+1$ and uses the last approximate from level N as an initial guess at the next finer level, i.e.

$$p_{N+1}^{0,\delta} := p_N^{k_*(N,\delta),\delta}.$$

Algorithm 2.1 summarizes the procedure.

Algorithm 2.1. *Iterative multilevel algorithm for modified Landweber iterations:*

SET $p_0^{0,\delta} := P_0 p^0 \in X_0$
SET $N = 0$
SET $k = 0$
SET $k_*(N,\delta) = 0$
CHOOSE $C_1 < C_2$ sufficiently large
WHILE $||F(p_N^{k_*(N,\delta),\delta}) - y^\delta|| > C_2\delta$
  $k = 0$
  If $N > 0$
    $p_{N+1}^{0,\delta} = p_N^{k_*(N,\delta),\delta}$
    $N = N + 1$
  DO WHILE $||F(p_N^{k,\delta}) - y^\delta||$ violates (2.10) or $k > \tilde{k}_{\max}(N)$
    $p_N^{k+1,\delta} = p_N^{k,\delta} + \omega_N^k s_N^{k,\delta}, \quad s_N^{k,\delta} := P_N F'(p_N^{k,\delta})^*(y^\delta - F(p_N^{k,\delta}))$
    where $\omega_N^{k,\delta}$ is either $\omega_N^{k,\delta} := \frac{||s_N^{k,\delta}||^2}{||F'(p_N^{k,\delta})s_N^{k,\delta}||^2}$
    or $\omega_N^{k,\delta} := \frac{||y^\delta - F(p_N^{k,\delta})||^2}{||s_N^{k,\delta}||^2}$
    $k = k + 1$
  $k_*(N,\delta) = k$
$p_{N_*(\delta)} := p_N^{k_*(N,\delta),\delta}$

The algorithm can analogously be formulated with (2.10) replaced by (2.11). The assumption that C_1 and C_2 are sufficiently large can be made more precise with the help of the following definition which is taken from [21]:

Definition 2.2. An operator F is called regular at level X_N in $\overline{U}_N := \overline{X_N \cap \mathcal{B}_\rho(p_0^0)}$ if it is Fréchet-differentiable in $\overline{U}_N := \overline{X_N \cap \mathcal{B}_\rho(p_0^0)} \subseteq D(F)$ and

$$B_{inf}(N, p^\dagger, p_0^0, \rho) := \inf_{p \in U_N, p \neq P_N p^\dagger} \frac{||F(p) - F(P_N p^\dagger)||}{||p - P_N p^\dagger||} > 0.$$

An operator F is called regular at level X_N in U_N with magnitude λ_N if it is regular at level X_N and

$$\lambda_N := B_{inf}(N, p^\dagger, p_0^0, \rho).$$

Here, λ_N measures the stability of the solution of (2.1) with respect to perturbations of the right-hand side data on the finite dimensional subspace X_N.
So for the constants the following is assumed if F is regular at level X_N with magnitude λ_N

$$C_1 \quad \geq \quad 4(1+\eta_N), \quad C_0 < C_1 < C_2 \tag{2.18}$$

with

$$\lambda_N \frac{C_0^2}{8(1+C_0)^2} \leq ||F'(p_N^{0,\delta})||, \quad \text{and } C_0 \geq \sqrt{8} \quad \forall N.$$

2.1. Convergence Results

Before we show monotonicity of the iterates on each level we prove the well-definedness of the step-length parameters $\omega_N^{k,\delta}$. One can show, that as long as the stopping rules as defined in (2.10) and (2.11) are not active, the parameter update $s_N^{k,\delta}$ and $F'(p_N^{k,\delta})s_N^{k,\delta}$ are nonzero.

Lemma 2.1. *Let $p^\dagger \in \mathcal{B}_{\rho/2}(p^0)$ be a solution of (2.1) and $\overline{k}_*(N,\delta)$ be as in (2.12) and $p_N^{k,\delta} - P_N p^\dagger \neq 0$ for all $k < \overline{k}_*(N,\delta)$. Then*

$$||s_N^{k,\delta}|| \neq 0 \quad \textit{and} \quad ||F'(p_N^{k,\delta})s_N^{k,\delta}|| \neq 0 \quad \textit{for all } \; k < \overline{k}_*(N,\delta).$$

Proof. We carry out the proof in case of (2.10). The case (2.11) then immediately follows, since by (2.3) the right hand side in (2.11) is greater or equal the one in (2.10) if $\tilde{C}_1 = C_1$.
If $\overline{k}_*(N,\delta) = 0$ we need not to prove anything. Otherwise (2.13) holds. Assume that $k < \overline{k}_*(N,\delta)$. If $F'(p_N^{k,\delta})^*(F(p_N^{k,\delta}) - y^\delta)$ would vanish, then

$$\begin{aligned} 0 \quad &= \quad \big(F(p_N^{k,\delta}) - y^\delta, F'(p_N^{k,\delta})(p_N^{k,\delta} - P_N p^\dagger)\big) \\ &= \quad \big(F(p_N^{k,\delta}) - y^\delta, F(p_N^{k,\delta}) - y^\delta\big) \\ &\quad + \big(F(p_N^{k,\delta}) - y^\delta, y - F(P_N p^\dagger)\big) \\ &\quad + \big(F(p_N^{k,\delta}) - y^\delta, y^\delta - y\big) \\ &\quad - \big(F(p_N^{k,\delta}) - y^\delta, F(p_N^{k,\delta}) - F(P_N p^\dagger) - F'(p_N^{k,\delta})(p_N^{k,\delta} - P_N p^\dagger)\big). \end{aligned}$$

From this we deduce

$$\begin{aligned} ||F(p_N^{k,\delta}) - y^\delta||^2 \quad &\leq \quad (\delta + ||y - F(P_N p^\dagger)||)||F(p_N^{k,\delta}) - y^\delta|| \\ &\quad + \eta_N \, ||F(p_N^{k,\delta}) - F(P_N p^\dagger)|| \, ||F(p_N^{k,\delta}) - y^\delta|| \end{aligned}$$

and further

$$\begin{aligned} ||F(p_N^{k,\delta}) - y^\delta|| \quad &\leq \quad \delta + ||y - F(P_N p^\dagger)|| \\ &\quad + \eta_N \left(||F(p_N^{k,\delta}) - y^\delta|| + ||y - F(P_N p^\dagger)|| + ||y - y^\delta|| \right). \end{aligned} \tag{2.19}$$

So

$$||F(p_N^{k,\delta}) - y^\delta|| \leq \frac{1+\eta_N}{1-\eta_N}(||F(P_N p^\dagger) - y|| + \delta)$$

which contradicts (2.13).
To show that $||F'(p_N^{k,\delta})s_N^{k,\delta}|| \neq 0$ let us assume again the contrary, i.e. $||F'(p_N^{k,\delta})s_N^{k,\delta}|| = 0$. Then $s_N^{k,\delta} \in \mathcal{N}(F'(p_N^{k,\delta})) = \{0\}$ which is a contradiction to the already shown fact $s_N^{k,\delta} \neq 0$. □

This actually guarantees that the choices of the relaxation parameters in (2.7) and (2.8) are well-defined. Now, monotonicity of the iteration error at a fixed level N will be proven:

Theorem 2.3. *Let $N \in \mathbb{N}_0$ be fixed such that $||(I - P_N)p^\dagger|| < \rho/2$, where $p^\dagger$ is a solution of (2.1) in $\mathcal{B}_{\frac{\rho}{2}}(p_N^{0,\delta})$ and $p_N^{0,\delta} \in X_N$. Assume that Algorithm 2.1 carries out at least one inner step at level N, i.e. there exists an iteration index $k \geq 0$ such that (2.13) and (2.14) hold respectively with $C_1 \geq 4(1+\eta_N)$. Then, for $0 \leq k < \overline{k}_*(N,\delta)$*

$$\begin{aligned} p_N^{k+1,\delta} \in \mathcal{B}_{\frac{\rho}{2}}(p^\dagger) \cap X_N \quad &\subseteq \quad \mathcal{B}_\rho(p_N^{0,\delta}) \cap X_N \quad \textit{further} \\ ||p^\dagger - p_N^{k+1,\delta}|| \quad &\leq \quad ||p^\dagger - p_N^{k,\delta}|| \quad \textit{and} \\ ||P_N p^\dagger - p_N^{k+1,\delta}|| \quad &\leq \quad ||P_N p^\dagger - p_N^{k,\delta}||. \end{aligned} \tag{2.20}$$

Proof. Let $p_N^{k,\delta} \in \mathcal{B}_{\frac{\rho}{2}}(p^\dagger)$ for $0 \leq k < \overline{k}_*(N,\delta)$. From the definition of the iteration it follows that

$$\begin{aligned} &||p_N^{k+1,\delta} - p^\dagger||^2 \\ &\quad = \quad ||p_N^{k,\delta} - p^\dagger||^2 + ||\omega_N^{k,\delta} P_N F'(p_N^{k,\delta})^*(F(p_N^{k,\delta}) - y^\delta)||^2 \\ &\qquad - 2\omega_N^{k,\delta} \left(F'(p_N^{k,\delta})(p_N^{k,\delta} - P_N p^\dagger), F(p_N^{k,\delta}) - y^\delta \right) \\ &\quad = \quad ||p_N^{k,\delta} - p^\dagger||^2 + ||\omega_N^{k,\delta} P_N F'(p_N^{k,\delta})^*(F(p_N^{k,\delta}) - y^\delta)||^2 \\ &\qquad + 2\omega_N^{k,\delta} \left(F(p_N^{k,\delta}) - F(P_N p^\dagger) - F'(p_N^{k,\delta})(p_N^{k,\delta} - P_N p^\dagger), F(p_N^{k,\delta}) - y^\delta \right) \\ &\qquad - 2\omega_N^{k,\delta} \left(F(p_N^{k,\delta}) - F(P_N p^\dagger), F(p_N^{k,\delta}) - y^\delta \right). \end{aligned}$$

With the nonlinearity condition (2.5) we obtain that

$$\begin{aligned}
&\Big(F(p_N^{k,\delta}) - F(P_N p^\dagger) - F'(p_N^{k,\delta})(p_N^{k,\delta} - P_N p^\dagger), F(p_N^{k,\delta}) - y^\delta\Big) \\
&\quad - \Big(F(p_N^{k,\delta}) - F(P_N p^\dagger), F(p_N^{k,\delta}) - y^\delta\Big) \\
&\leq \eta_N ||F(p_N^{k,\delta}) - F(P_N p^\dagger)||\, ||F(p_N^{k,\delta}) - y^\delta|| \\
&\quad - \Big(F(p_N^{k,\delta}) - y^\delta, F(p_N^{k,\delta}) - y^\delta\Big) \\
&\quad + ||y^\delta - F(P_N p^\dagger)||\, ||F(p_N^{k,\delta}) - y^\delta|| \\
&\leq\ (\eta_N - 1)||F(p_N^{k,\delta}) - y^\delta||^2 + (1+\eta_N)||y^\delta - F(P_N p^\dagger)||\, ||F(p_N^{k,\delta}) - y^\delta||.
\end{aligned}$$

By (2.13)

$$\begin{aligned}
&(1+\eta_N)||y^\delta - F(P_N p^\dagger)||\, ||F(p_N^{k,\delta}) - y^\delta|| \\
&\leq (1+\eta_N)\left(||y - F(P_N p^\dagger)|| + \delta\right) ||F(p_N^{k,\delta}) - y^\delta|| \leq \frac{1}{4}||F(p_N^{k,\delta}) - y^\delta||^2.
\end{aligned} \tag{2.21}$$

Hence we continue to estimate

$$\begin{aligned}
||p_N^{k+1,\delta} - p^\dagger||^2 \quad &\leq \quad ||p_N^{k,\delta} - p^\dagger||^2 + (\omega_N^{k,\delta})^2 ||s_N^{k,\delta}||^2 \\
&\quad + 2\omega_N^{k,\delta}(\eta_N - \frac{3}{4})||F(p_N^{k,\delta}) - y^\delta||^2.
\end{aligned}$$

Finally, it holds that

$$\begin{aligned}
&||p_N^{k+1,\delta} - p^\dagger||^2 + 2\omega_N^{k,\delta}(\frac{1}{4} - \eta_N)||F(p_N^{k,\delta}) - y^\delta||^2 \\
&\quad \leq ||p_N^{k,\delta} - p^\dagger||^2 + (\omega_N^{k,\delta})^2 ||s_N^{k,\delta}||^2 - \omega_N^{k,\delta}||F(p_N^{k,\delta}) - y^\delta||^2.
\end{aligned} \tag{2.22}$$

Inserting now the choice of $\omega_N^{k,\delta}$ as a minimal error method (2.8) one sees, that the difference of the last two terms on the RHS of (2.22) vanishes. For the steepest descent variant (2.7) it holds

$$\omega_N^{k,\delta}||s_N^{k,\delta}||^2 = \frac{\Big(F'(p_N^{k,\delta})s_N^{k,\delta}, F(p_N^{k,\delta}) - y^\delta\Big)^2}{||F'(p_N^{k,\delta})s_N^{k,\delta}||^2} \leq ||F(p_N^{k,\delta}) - y^\delta||^2,$$

so in both cases

$$||p_N^{k+1,\delta} - p^\dagger||^2 + 2\omega_N^{k,\delta}(\frac{1}{4} - \eta_N)||F(p_N^{k,\delta}) - y^\delta||^2 \leq ||p_N^{k,\delta} - p^\dagger||^2. \tag{2.23}$$

The monotonicity of $||P_N p^\dagger - p_N^{k,\delta}||$ follows by inspection of the estimations of this proof. □

The next lemma will show that the first Landweber step at the next finer level under certain assumptions always provides some improvement to the old state of the unknown. Whereas the results so far hold for both stopping rules (2.10) and (2.11), we restrict ourselves to (2.11) with (2.16) now.

Lemma 2.2. *Let F be regular at level X_N with magnitude λ_N in U_N and assume that $\eta_N \leq \frac{1}{8}$, further that (2.14) holds for $k = 0$ at level $N+1$. Then with $\psi := \frac{\hat{C}_1^2}{8(1+\hat{C}_1)^2}$ and $\hat{C}_1 \geq \sqrt{8}$*

$$||p_{N+1}^{1,\delta} - P_{N+1}p^\dagger||^2 \leq (1 - \omega_{N+1}^{0,\delta}\psi\lambda_N^2)||p_{N+1}^{0,\delta} - P_N p^\dagger||^2.$$

Proof. Let us start with some estimates at level N. Suppose $p_N^{k,\delta}, P_N p^\dagger \in \mathcal{B}_\rho(p_0^0)$, then it follows from (2.3) for $k \leq k_*(N,\delta)$

$$\begin{aligned} ||F(p_N^{k,\delta}) - y^\delta|| &\geq ||F(p_N^{k,\delta}) - F(P_N p^\dagger)|| - ||F(P_N p^\dagger) - y|| - \delta \\ &\geq ||F(p_N^{k,\delta}) - F(P_N p^\dagger)|| - (||P_N p^\dagger - p^\dagger|| + \delta). \end{aligned}$$

Now

$$||F(p_N^{k,\delta}) - F(P_N p^\dagger)|| \leq \left(1 + \frac{1}{\hat{C}_1}\right) ||F(p_N^{k,\delta}) - y^\delta|| \tag{2.24}$$

and so together with (2.14) for $k = 0$ and since $\max\{a,b\}^2 \geq \frac{1}{2}a^2 + \frac{1}{2}b^2$

$$||F(p_N^{0,\delta}) - y^\delta||^2 \geq \frac{\hat{C}_1^2}{2(1+\hat{C}_1)^2}||\mathrm{F}(p_N^{0,\delta}) - F(P_N p^\dagger)||^2 + \frac{\hat{C}_1^2}{2}||(P_N - I)p^\dagger||^2. \tag{2.25}$$

Further $\psi \leq \left(\frac{1}{2} - 2\eta_{N+1}\right)\frac{\hat{C}_1^2}{2(1+\hat{C}_1)^2}$ and $\psi_1 := \frac{\hat{C}_1^2}{8} \leq \left(\frac{1}{2} - 2\eta_{N+1}\right)\frac{\hat{C}_1^2}{2}$.
From the proof of monotonicity (2.23) with $p^\dagger$ replaced by $P_N p^\dagger$, due to orthogonality, and since $p_{N+1}^{0,\delta} = p_N^{k_*(N,\delta),\delta} \in X_N \subseteq X_{N+1}$ one obtains

$$\begin{aligned} &||p_{N+1}^{1,\delta} - P_{N+1}p^\dagger||^2 + \omega_{N+1}^{0,\delta}\left(\frac{1}{2} - 2\eta_{N+1}\right)||F(p_{N+1}^{0,\delta}) - y^\delta||^2 \\ \leq\ & ||p_{N+1}^{0,\delta} - P_{N+1}p^\dagger||^2 \\ \leq\ & ||p_{N+1}^{0,\delta} - P_N p^\dagger||^2 + ||P_{N+1}p^\dagger - P_N p^\dagger||^2 \end{aligned}$$

from which with (2.24) and (2.25) follows

$$\begin{aligned} &||p_{N+1}^{1,\delta} - P_{N+1}p^\dagger||^2 + \omega_{N+1}^{0,\delta}\psi||F(p_{N+1}^{0,\delta}) - F(P_N p^\dagger)||^2 \\ &\qquad + \omega_{N+1}^{0,\delta}\psi_1||P_N p^\dagger - p^\dagger||^2 \\ \leq\ & ||p_{N+1}^{0,\delta} - P_N p^\dagger||^2 + ||P_{N+1}p^\dagger - P_N p^\dagger||^2. \end{aligned} \tag{2.26}$$

Now, with the boundedness (2.9) of $\omega_{N+1}^{0,\delta}$ from below as well as $\psi_1 \geq 1$ and by orthogonality

$$\begin{aligned} ||P_N p^\dagger - p^\dagger||^2 &= ||P_N p^\dagger - P_{N+1}p^\dagger + P_{N+1}p^\dagger - p^\dagger||^2 \\ &= ||P_N p^\dagger - P_{N+1}p^\dagger||^2 + ||P_{N+1}p^\dagger - p^\dagger||^2 \\ &\quad +2\left(P_N p^\dagger - P_{N+1}p^\dagger, P_{N+1}p^\dagger - p^\dagger\right) \\ &\geq ||P_N p^\dagger - P_{N+1}p^\dagger||^2 \end{aligned}$$

we get

$$||(P_{N+1} - P_N)p^\dagger||^2 \leq \omega_{N+1}^{0,\delta}\psi_1||(P_N - I)p^\dagger||^2.$$

Consequently (2.26) reduces to

$$||p_{N+1}^{1,\delta} - P_{N+1}p^\dagger||^2 + \omega_{N+1}^{0,\delta}\psi||F(p_{N+1}^{0,\delta}) - F(P_N p^\dagger)||^2 \leq ||p_{N+1}^{0,\delta} - P_N p^\dagger||^2. \quad (2.27)$$

From the assumption that F is regular at level N with magnitude λ_N and with $p_{N+1}^{0,\delta} = p_N^{k_*(N,\delta),\delta} \in \mathcal{B}_\rho(p_N^{0,\delta})$ one has

$$||F(p_{N+1}^{0,\delta}) - F(P_N p^\dagger)|| \geq \lambda_N||p_{N+1}^{0,\delta} - P_N p^\dagger||.$$

From the latter inequality it follows that

$$||p_{N+1}^{1,\delta} - P_{N+1}p^\dagger||^2 \leq (1 - \omega_{N+1}^{0,\delta}\psi\lambda_N^2)||p_{N+1}^{0,\delta} - P_N p^\dagger||^2. \quad (2.28)$$

□

Corollary 2.3. *Let the assumptions from Lemma 2.2 hold. Then for all $k < k_*(N,\delta)$:*

$$||p_{N+1}^{k+1,\delta} - P_{N+1}p^\dagger||^2 \leq (1 - \omega_N^{0,\delta}\psi\lambda_N^2)||p_N^{0,\delta} - P_N p^\dagger||^2.$$

Proof. With the results from Theorem 2.3 and Lemma 2.2 it holds

$$\begin{aligned} ||p_{N+1}^{k+1,\delta} - P_{N+1}p^\dagger||^2 &\leq ||p_{N+1}^{1,\delta} - P_{N+1}p^\dagger||^2 \\ &\leq (1 - \omega_{N+1}^{0,\delta}\psi\lambda_N^2)||p_{N+1}^{0,\delta} - P_N p^\dagger||^2 \\ &= (1 - \omega_{N+1}^{0,\delta}\psi\lambda_N^2)||p_N^{k_*(N,\delta),\delta} - P_N p^\dagger||^2 \\ &\leq (1 - \omega_{N+1}^{0,\delta}\psi\lambda_N^2)||p_N^{0,\delta} - P_N p^\dagger||^2. \end{aligned}$$

□

Now we have all auxiliary means for deriving the main result of this article. It states that the iterates of the proposed multilevel algorithm with least squares or minimal error inner iterations form a monotone sequence.

We define now a set which contains the indices of those levels where at least one iteration is performed and where (2.17) is not active yet

$$\hat{\mathcal{N}}^\delta := \{N < N_*(\delta) \mid ||F(p_N^{0,\delta}) - y^\delta|| > C_1(\delta + ||(I - P_N)p^\dagger||)\} =: (N_l)_{l=1}^L \quad (2.29)$$

Theorem 2.4. *Let all conditions of Lemma 2.2 hold. If for all $N \in \hat{\mathcal{N}}^\delta$ the operator F is regular at level N with magnitude λ_N in $U_N = X_N \cap \mathcal{B}_\rho(p_N^0)$, then for all $N < N_*(\delta)$ and all $k \leq k_*(N,\delta)$*

$$||p_{N+1}^{k+1,\delta} - P_{N+1}p^\dagger||^2 \leq \prod_{\substack{I \in \hat{\mathcal{N}}^\delta \\ I \leq N}} (1 - \omega_{I+1}^{0,\delta}\psi\lambda_I^2)||p_0^{0,\delta} - P_0 p^\dagger||^2. \tag{2.30}$$

Especially, if additionally for all $l \in \{1, ..., L_* - 1\}$

$$(1 - \omega_{N_{l+1}}^{0,\delta}\psi\lambda_{N_l}^2)\frac{\phi(\lambda_{N_l})}{\phi(\lambda_{N_{l+1}})} \leq 1 \tag{2.31}$$

holds with some function $\phi : \mathbb{R} \to \mathbb{R}$, then

$$||p_{N_*(\delta)} - P_{N_*(\delta)}p^\dagger||^2 \leq ||p_0^{0,\delta} - P_0 p^\dagger||^2 \, \frac{\phi(\lambda_{N_{L_*}})}{\phi(\lambda_{N_1})}. \tag{2.32}$$

In case $\hat{\mathcal{N}}^\delta = \{0, ..., N_*(\delta)\}$ this yields

$$||p_{N_*(\delta)} - P_{N_*(\delta)}p^\dagger|| = \mathcal{O}(\sqrt{\phi(\lambda_{N_*(\delta)})}). \tag{2.33}$$

Proof. The result in (2.30) directly follows from Corollary 2.3. Inserting $N := N_*(\delta) - 1,\ k = k_*(N_*(\delta), \delta)$ and (2.31) into (2.30) we get

$$\begin{aligned} & ||p_{N_*}(\delta) - P_{N_*(\delta)}p^\dagger||^2 \\ \leq & \prod_{l=1}^{L_*}(1 - \omega_{N_{l+1}}^{0,\delta}\psi\lambda_{N_l}^2)||p_0^{0,\delta} - P_0 p^\dagger||^2 \\ \leq & \prod_{l=1}^{L_*-1}\frac{\phi(\lambda_{N_{l+1}})}{\phi(\lambda_{N_l})}||p_0^{0,\delta} - P_0 p^\dagger||^2 \\ = & \frac{\phi(\lambda_{N_{L_*}})}{\phi(\lambda_{N_1})}||p_0^{0,\delta} - P_0 p^\dagger||^2. \end{aligned} \tag{2.34}$$

□

As opposed to [21], Lemma 5.4, this can give a convergence rate not only for mildly-ill posed but also for exponentially ill-posed problems for example with $\phi(\cdot) \sim \log(\cdot)$.

2.2. Convergence in Case of Exact Data

It is also of interest to provide weak convergence results in case of noise free data. These results will e.g. be used later on when the regularization property of the multi-level algorithm will be shown. At this point we introduce the following set

$$\mathcal{N}^\delta := \{N \in \mathbb{N} \ : \ ||F(p_N^{0,\delta}) - y|| > C_1(\delta + ||F(P_N p^\dagger) - y^\delta||)\} \tag{2.35}$$

which contains all levels where at least one inner iterations is performed, so that $p_N^{1,\delta}$ is certainly computed.

Proposition 2.4. *If $\delta = 0$ and $k_*(N,\delta)$ as in (2.16)*

$$F(p_N^{k_*(N,0),0}) \to y \quad \textit{as} \quad N \to \infty. \tag{2.36}$$

Proof. There are two cases to be considered:
1) The iteration stops at a finite level N. In this situation by (2.17) the last iterate is a solution of (2.1).
2) The iteration does not terminate. Because of (2.23) it holds that

$$\sum_{I \in \mathcal{N}^0} \sum_{j=0}^{k_*(I,0)-1} ||y - F(p_I^{j,0})||^2 < \infty. \tag{2.37}$$

For $I \notin \mathcal{N}^0$ the following is true

$$\begin{aligned} ||y - F(p_I^{0,0})|| &\leq ||F(P_I p^\dagger) - y|| \quad \text{or} \\ ||y - F(p_I^{0,0})|| &\leq ||(I - P_I)p^\dagger||. \end{aligned} \tag{2.38}$$

Now, we will make use of a subsequence-subsequence argument applied to

$$a_N := ||y - F(p_N^{0,0})||.$$

Let $(a_{N_i})_{i\in\mathbb{N}}$ be an arbitrary subsequence. We distinguish between the cases:

a) The index set $\mathcal{N}^0 \cap \{N_i\}_{i\in\mathbb{N}}$ is infinite, hence we can denote it by $(N_{i_l})_{l\in\mathbb{N}}$. Due to (2.37) $(a_{N_i})_{i\in\mathbb{N}}$ converges to zero.

b) The set $\mathcal{N}^0 \cap (N_i)_{i\in\mathbb{N}}$ is finite, then $(\mathbb{N} \setminus \mathcal{N}^0) \cap \{N_i\}_{i\in\mathbb{N}}$ must be infinite and with $(N_{i_l})_{l\in\mathbb{N}} := (\mathbb{N} \setminus \mathcal{N}^0) \cap \{N_i\}_{i\in\mathbb{N}}$, we have convergence of $(a_{N_{i_l}})_{l\in\mathbb{N}}$ to zero by pointwise convergence of P_I to the identity in (2.4).

So, in both cases, $(a_{N_i})_{i\in\mathbb{N}}$ has a subsequence converging to zero. This implies that each subsequence of $(a_N)_{N\in\mathbb{N}}$ has a convergent subsequence and the limit of each convergent subsequence of $(a_N)_{N\in\mathbb{N}}$ is zero.

□

With the latter result weak convergence for exact data can be established:

Proposition 2.5. *Let $\delta = 0$ and the assumptions of Proposition 2.4 hold. Moreover, let F be weakly closed. Then each subsequence of $p_N^{k_*(N,0),0}$ has a weakly convergent subsequence and each weak accumulation point is a solution of $F(p) = y$. If the solution $p^\dagger$ of (2.1) is unique, then $p_N^{k_*(N,0),0}$ converges weakly to $p^\dagger$.*

Proof. In case Algorithm 2.1 terminates after a finite number $N_*(0)$ of iterations by the stopping criterion (2.17) then $p_{N_*(0)}$ solves (2.1). Otherwise if $k_*(N,0) > 0$ it follows from Theorem 2.3 that

$$||p^\dagger - p_N^{k_*(N,0),0}|| \leq ||p^\dagger - p_0^{0,0}||$$

which trivially holds in the complementary case $k_*(N,0) = 0$. Therefore, we have boundedness of $p_N^{k_*(N,0),0}$ in X and $p_N^{k_*(N,0),0}$ has a weakly convergent subsequence. From (2.36) and the weak closedness of the operator F it follows that for each weak accumulation point $\overline{z}$, the identity $F(\overline{z}) = y$ holds, which proves the assertion. □

2.3. Regularization Property

A still open question is whether the iterative multilevel algorithm has regularizing properties or not, i.e. if it converges to the exact solution in case that the data error level forms a sequence converging to zero. In order to answer this question we start at with fixed iteration index k and fixed level N,

Theorem 2.5. *Let $\{\delta_n\} \to 0$ for $n \to \infty$. Further, denote by y^{δ_n} a sequence of noisy data and assume that F' is Lipschitz continuous. Then, for fixed $k \in \mathbb{N}$*

$$p_N^{k,\delta_n} \to p_N^k, \quad \text{as } n \to \infty, \tag{2.39}$$

where $p_N^{k,\delta_n} := p_N^{k_*(N,\delta_n),\delta_n}$ for $k \geq k_*(N,\delta_n)$.

Proof. For each pair (δ_n, y^{δ_n}) let us denote by $k_*(N,\delta_n)$ the corresponding stopping index according to (2.17). Similar as in [20] one can define for each level N

$$f_N^k(n) := ||F(p_N^{k,\delta_n}) - y^{\delta_n}||$$

and prove (2.39) by induction for N and k:

1. $N = 0$ and $k = 0$: Since $p_0^{0,\delta_n} = P_0 p^0$ it clearly depends continuously on y^{δ_n}.

2. $N = 0$ and $k \to k+1$. Let $k \in \mathbb{N}$ be fixed and suppose that $p_0^{k,\delta_n} \to p_0^k$ as $\delta_n \to 0$. Assuming that $f_0^k(n)$ is monotone (otherwise consider monotone subsequences) one needs to consider the two cases:

1. $f_0^k(n)$ is strictly bounded from below. Then for $n \to \infty$,
$f_0^k(n) \to ||F(p_0^k) - y|| > C_1||(I - P_0)p^\dagger|| > 0$ and according to Lemma 2.1 stating that $s_0^k \neq 0$

$$||F'(p_0^k)F'(p_0^k)^*(F(p_0^k) - y)|| > 0, \quad ||F'(p_0^k)^*(F(p_0^k) - y)|| > 0$$

which implies continuous dependence of ω_0^k in both cases (2.7) and (2.8). From the definition of the modified Landweber iteration, continuity of F and Lipschitz continuity of F' it follows that $p_0^{k+1,\delta_n} \to p_0^{k+1}$ for $n \to \infty$.

2. Let $f_0^k(n) \to 0$: Then $f_0^k(n) \to ||F(p_0^k) - y|| = 0$ for $n \to \infty$, i.e. p_0^k solves (2.1) The following two situations need to be distinguished:
b.i) $f_0^k(n) > C_2\delta_n$, then $k < \overline{k}_*(0, \delta_n)$ and substituting $p^\dagger$ by p_0^k in (2.20)

$$||p_0^k - p_0^{k+1,\delta_n}|| \leq ||p_0^k - p_0^{k,\delta_n}||.$$

b.ii) $f_0^k(n) \leq C_2\delta_n$, then the iteration is stopped and $p_0^{k+1,\delta_n} = p_0^{k,\delta_n}$. Together (b.i) and (b.ii) give $p_0^{k+1,\delta_n} \to p_0^k = p_0^{k+1}$ for $n \to 0$.

Now, assume that for some $N > 0$ one has shown that p_N^{k+1,δ_n} depends continuously on the data. Then $p_{N+1}^{0,\delta_n} = p_N^{k_*(N,\delta_n),\delta_n}$ does since $\overline{k}_*(N, \delta_n)$ continuously depends on the data and therefore equals some $k_*(N)$ for all $n \geq n_0$ with n_0 sufficiently large and one can argue as above to carry out the induction step $N \to N + 1$. □

The next result shows that the Algorithm 2.1 with its stopping rules is a regularizing method. For a sequence of data errors which is converging to zero, the regularized solution of (2.1) converges to the exact one $p^\dagger$.

Theorem 2.6. *Assume that δ_n forms a sequence of data errors converging to zero and that the assumptions of Theorem 2.5 are satisfied. Then, the sequence $p_{N_*(\delta_n)}^{\delta_n}$ converges weakly subsequentially (in the sense of Proposition 2.5) to the solution of (2.1).*

Proof. We consider the two cases for $N_*(\delta_n)$:

1.) In the first case we assume that $N_*(\delta_n)$ has a finite accumulation point N for $n \to \infty$. Without loss of generality, $N_*(\delta_n) = N$ for all n sufficiently large. By (2.16) it is assured that $k_*(N, \delta_n)$ has a finite accumulation point. Now, without loss of generality assume that $k_*(N, \delta_n) = k$ for all n sufficiently large. By definition of $k_*(N, \delta_n)$ it follows that

$$||y^{\delta_n} - F(p_N^{k,\delta_n})|| \leq \tau\delta_n. \tag{2.40}$$

Since by Theorem 2.5 $p_N^{k,\delta} \to p_N^k$ for $y^\delta \to y$ as k is fixed now, one has

$$p_N^{k,\delta_n} \to p_N^k \tag{2.41}$$

and

$$F(p_N^{k,\delta_n}) \to F(p_N^k).$$

Taking the limit in (2.40) gives $F(p_N^k) = y$.

2.) In the second case where $N_*(\delta_n) \to \infty$ for $n \to \infty$, then

$$p_M^{k_*(M,\delta_n),\delta_n} = p_{M+1}^{0,\delta_n} \to p_{M+1}^0 \quad \text{for } n \to \infty \tag{2.42}$$

since $k = 0$ is fixed and by an application of Theorem 2.5. Hence Proposition 2.5 yields weak subsequential convergence in this case.

The proof is complete. □

Note, that in the proof of Theorem 2.6 the case that $k_*(N, \delta_n) \to \infty$ as $n \to \infty$ will not occur due to (2.15) and (2.16).

3. The Piezoelectric Parameter Curve Identification Problem

We formulate the inverse problem of identifying the material parameter curves from time dependend electrical or mechanical measurements with the following parameter-to-solution map F which in its most general form is given by

$$\begin{aligned} F : \mathcal{D}(F) \subseteq X_{par} &\rightarrow Y_{meas} \\ (\mathbf{c}^E, \mathbf{e}, \boldsymbol{\varepsilon}^S) &\mapsto y^\delta(t), \quad t \in [0,T], \end{aligned} \tag{3.1}$$

where $(\mathbf{c}^E, \mathbf{e}, \boldsymbol{\varepsilon}^S)$ are parameter curves depending on the physical field quantities electric field and mechanical strain. In order to reduce the complexity of computations and the representation of the Fréchet derivative of F and its adjoint we consider only the dependency of the 33 components of $\mathbf{e}$ and $\boldsymbol{\varepsilon}^S$ on $\vec{E}_3 = (0,0,\phi_{|3})^T$ and assume that the constant material parameters are sufficiently precisely known, e.g. by applying means suggested in [6] or by performing simulation-based material parameter identification for the linear case, see [8, 14]. The parameter-to-solution map reduces and specifies in case of electric charge measurements to

$$\begin{aligned} F : \mathcal{D}(F) \subseteq \left(H^2(\underline{\phi_{|3}}, \overline{\phi_{|3}})\right)^2 &\rightarrow L^2([0,T]) \\ (e_{33}, \varepsilon_{33}) &\mapsto \int_\Gamma \vec{D}(t) \cdot \vec{n} d\Gamma \\ &= \int_\Gamma \left(\mathbf{e}_3(\phi_{|3})\mathbf{B}\mathbf{u}(t) - \boldsymbol{\varepsilon}_3^S(\phi_{|3})\nabla\phi(t)\right) \cdot \vec{n} d\Gamma, \end{aligned} \tag{3.2}$$

where the pair $(\mathbf{u}, \phi)$ solves

$$\begin{aligned} \rho\frac{\partial^2 \mathbf{u}}{\partial t^2} - \mathbf{B}^T\left(\mathbf{c}^E\mathbf{B}\mathbf{u} + \mathbf{e}_3(\phi_{|3})^T\nabla\phi\right) &= 0 \quad \text{in } \Omega \times [0,T] \\ -\nabla \cdot \left(\mathbf{e}_3(\phi_{|3})\mathbf{B}\mathbf{u} - \boldsymbol{\varepsilon}_3^S(\phi_{|3})\nabla\phi\right) &= 0 \quad \text{in } \Omega \times [0,T], \end{aligned} \tag{3.3}$$

combined with the boundary and initial conditions

$$\begin{aligned} \mathbf{N}^T(\mathbf{c}^E\mathbf{B}\mathbf{u} + \mathbf{e}_3(\phi_{|3})^T\nabla\phi\big) &= 0 \quad \text{on } \partial\Omega \times [0,T] \\ \phi &= 0 \quad \text{on } \Gamma_g \times [0,T] \\ \phi &= \phi^e \quad \text{on } \Gamma_e \times [0,T] \\ \left(\mathbf{e}_3(\phi_{|3})\mathbf{B}\mathbf{u} - \boldsymbol{\varepsilon}_3^S(\phi_{|3})\nabla\phi\right) \cdot \vec{n} &= 0 \quad \text{on } \Gamma_r \times [0,T] \\ \mathbf{u}(\cdot,0) &= \mathbf{u}_0 \quad \text{on } \Omega \\ \mathbf{u}_t(\cdot,0) &= \dot{\mathbf{u}}_0 \quad \text{on } \Omega \end{aligned} \tag{3.4}$$

and the tensors $\mathbf{e}_3(v), \boldsymbol{\varepsilon}_3^S(v)$ and $\mathbf{c}^E$ are defined as

$$\begin{aligned}
\mathbf{e}_3(v) &= \begin{pmatrix} 0 & 0 & 0 & 0 & e_{15} & 0 \\ 0 & 0 & 0 & e_{15} & 0 & 0 \\ e_{31} & e_{31} & e_{33}(v) & 0 & 0 & 0 \end{pmatrix}, \\
\boldsymbol{\varepsilon}_3^S(v) &= \begin{pmatrix} \varepsilon_{11} & 0 & 0 \\ 0 & \varepsilon_{11} & 0 \\ 0 & 0 & \varepsilon_{33}(v) \end{pmatrix} \text{ and } \mathbf{c}^E := \begin{pmatrix} c_{11}^E & c_{12}^E & c_{13}^E & 0 & 0 & 0 \\ c_{12}^E & c_{11}^E & c_{13}^E & 0 & 0 & 0 \\ c_{13}^E & c_{13}^E & c_{33}^E & 0 & 0 & 0 \\ 0 & 0 & 0 & c_{44}^E & 0 & 0 \\ 0 & 0 & 0 & 0 & c_{44}^E & 0 \\ 0 & 0 & 0 & 0 & 0 & c_{66}^E \end{pmatrix}.
\end{aligned} \tag{3.5}$$

The derivatives of the terms in (3.5) are defined as

$$\mathbf{e}_3'(v) := \begin{pmatrix} 0 & 0 & 0 & 0 & 0 & 0 \\ 0 & 0 & 0 & 0 & 0 & 0 \\ 0 & 0 & e_{33}'(v) & 0 & 0 & 0 \end{pmatrix} \text{ and } \boldsymbol{\varepsilon}_3^{S\prime}(v) := \begin{pmatrix} 0 & 0 & 0 \\ 0 & 0 & 0 \\ 0 & 0 & \varepsilon_{33}^{S\,\prime}(v) \end{pmatrix}.$$

The choice of a second order Sobolev space as a pre-image space is motivated by the continuous differentiability of the parameter curves that is required for carrying out Newton's method in forward computations. Since we only have measurements of zero order derivatives available, i.e. electric charge or mechanical displacements and not any values of higher order derivatives with respect to time (velocity, acceleration or electric current) the data space is

$$Y = L^2[0,T]. \tag{3.6}$$

For the sought-after quantities, the parameter curves, as already mentioned, we assume spaces

$$\mathcal{D}(F) := X \subseteq (H^2(\underline{\phi_{|3}}, \overline{\phi_{|3}}))^2 \tag{3.7}$$

in order to obtain C^1 curves by *Sobolev's embedding theorem*. The operator F actually maps into $C^2[0,T]$. So we have a difference in the regularity of these spaces which corresponds to an ill-posedness of twice numerical differentiation for the parameter curves reconstruction, see e.g. Example 1.1 and 1.6 in [2].

3.1. The Adjoint Operator

The following is devoted to the computation of the adjoint operator of the linearized problem.

Proposition 3.1. *The adjoint operator $F'(e_{33},\varepsilon_{33}^S)^*$ of the linearization of F defined in (3.2) is given by*

$$\begin{aligned}&(F'(e_{33},\varepsilon_{33}^S)^*[z])(\lambda) \qquad (3.8)\\ =\quad &\int_0^T\int_\Omega \Phi(\lambda-\phi_{|3})\begin{pmatrix}(\mathbf{Bu})_3\tilde{z}_{|3}-\phi_{|3}(\mathbf{B}\tilde{v})_3\\ \phi_{|3}\tilde{z}_{|3}\end{pmatrix} d\Omega\, dt,\end{aligned}$$

where Φ is defined by

$$\Phi(a)=\frac{1}{2}\sqrt{\frac{\pi}{2}}(1+|a|)e^{-|a|}. \qquad (3.9)$$

The values $(\tilde{v},\tilde{z})$ are here obtained by solving the adjoint set of differential equations

$$\begin{aligned}\rho\tilde{v}_{tt}-\mathbf{B}^T(\mathbf{c}^E\mathbf{B}\tilde{v}+\mathbf{e}_3(\phi_{|3})^T\nabla\tilde{z}) &= 0 \text{ on } \Omega\times[0,T]\\ -\nabla\cdot\Big((\mathbf{e}_3(\phi_{|3})+\mathbf{e}_3'(\phi_{|3})\phi_{|3})\mathbf{B}\tilde{v}+\mathbf{e}_3'(\phi_{|3})\mathbf{B}\mathbf{u}\tilde{z}_{|3}&\\ -(\boldsymbol{\varepsilon}_3^{S'}(\phi_{|3})\phi_{|3}+\boldsymbol{\varepsilon}_3^S(\phi_{|3}))\nabla\tilde{z}\Big) &= 0 \text{ on } \Omega\times[0,T]\\ \mathbf{N}^T\Big(\mathbf{c}^E\mathbf{B}\tilde{v}+\mathbf{e}_3(\phi_{|3})^T\nabla\tilde{z}\Big) &= 0 \quad \text{on } \partial\Omega\times[0,T]\\ \tilde{z} &= z(t) \quad \text{on } \Gamma_e\times[0,T]\\ \tilde{z} &= 0 \quad \text{on } \Gamma_g\times[0,T]\\ \Big((\mathbf{e}_3(\phi_{|3})+\mathbf{e}_3'(\phi_{|3})\phi_{|3})\mathbf{B}\tilde{v}+\mathbf{e}_3'(\phi_{|3})\mathbf{B}\mathbf{u}\tilde{z}_{|3}&\\ -(\boldsymbol{\varepsilon}_3^{S'}(\phi_{|3})\phi_{|3}+\boldsymbol{\varepsilon}_3^S(\phi_{|3}))\nabla\tilde{z}\Big)\cdot\vec{n} &= 0 \quad \text{on } \Gamma_r\times[0,T]\\ \tilde{v}(\cdot,t=T)=\tilde{v}_t(\cdot,t=T) &= 0 \quad \text{on } \Omega. \qquad (3.10)\end{aligned}$$

By the analytic formula of the adjoint the smoothing character of the adjoint and so the ill-posedness of the linearized problem can be quantified by the following theorem:

Proposition 3.2. *Assume that the solution operator $S:z\mapsto(\tilde{v},\tilde{z})$ of the adjoint equation in (3.10) is bounded in its norm, i.e.*

$$||S||_{(H^\sigma(0,T))^*\to(H^\sigma(0,T;H^1_{0,\Gamma}(\Omega)^*))^*\times(H^\sigma(0,T;H^1_{\mathbf{B}}(\Omega)^*))^*}<\infty. \qquad (3.11)$$

If further $\mathbf{u},\phi\in C^\infty([0,T]\times\Omega)$, then the operator $F'(e_{33},\varepsilon_{33}^S)^*$ can be extended to a continuous linear operator from $(H^\sigma[0,T])^*$ to $(H^2(\mathbb{R}))^2$ for any $\sigma\in(0,3/2)$.

Proof. For any $z \in L^2[0,T]$ and $\sigma \in (1, \frac{3}{2})$ we have

$$
\begin{aligned}
&||F'(e_{33}, \varepsilon_{33}^S)^*[z]||_{(H^2(\mathbb{R}))^2} \\
&= \int_{\mathbb{R}} (1+\omega^2)^2 \left| \int_0^T \int_\Omega e^{-i\phi_{|3}\omega} (\mathcal{F}\mathbf{\Phi})(\omega) \begin{pmatrix} (\mathbf{Bu})_3 \tilde{z}_{|3} - \phi_{|3} (\mathbf{B}\tilde{v})_3 \\ \phi_{|3} \tilde{z}_{|3} \end{pmatrix} d\mathbf{\Omega}\ dt \right|^2 d\omega \\
&= \int_{\mathbb{R}} \left| \int_0^T \int_\Omega \frac{e^{-i\phi_{|3}\omega}}{1+\omega^2} \begin{pmatrix} (\mathbf{Bu})_3 \tilde{z}_{|3} - \phi_{|3} (\mathbf{B}\tilde{v})_3 \\ \phi_{|3} \tilde{z}_{|3} \end{pmatrix} d\mathbf{\Omega}\ dt \right|^2 d\omega \\
&= \int_{\mathbb{R}} \left(\frac{1}{1+\omega^2} \right)^2 \left(\left| \int_0^T \int_\Omega e^{-i\phi_{|3}\omega} \left((\mathbf{Bu})_3 \tilde{z}_{|3} - \phi_{|3} (\mathbf{B}\tilde{v})_3 \right) d\mathbf{\Omega} dt \right|^2 \right) d\omega \\
&\quad + \int_{\mathbb{R}} \left(\frac{1}{1+\omega^2} \right)^2 \left(\left| \int_0^T \int_\Omega e^{-i\phi_{|3}\omega} \phi_{|3} \tilde{z}_{|3}\, d\mathbf{\Omega} dt \right|^2 \right) d\omega \\
&\leq \int_{\mathbb{R}} \left(\frac{1}{1+\omega^2} \right)^2 \big(2||\tilde{z}_{|3}||^2_{(H^\sigma([0,T];L^2(\Omega)))^*} ||e^{-i\phi_{|3}\omega} (\mathbf{Bu})_3||^2_{H^\sigma([0,T];L^2(\Omega))} \\
&\quad + 2||(\mathbf{B}\tilde{v})_3||^2_{(H^\sigma([0,T];L^2(\Omega)))^*} ||e^{-i\phi_{|3}\omega} \phi_{|3}||^2_{H^\sigma([0,T];L^2(\Omega))} \\
&\quad + 2||\tilde{z}_{|3}||^2_{(H^\sigma([0,T];L^2(\Omega)))^*} ||e^{-i\phi_{|3}\omega} \phi_{|3}||^2_{H^\sigma([0,T];L^2(\Omega))} \big)\ d\omega. \qquad (3.12)
\end{aligned}
$$

We now analyze single components of (3.12), where

$$
\begin{aligned}
||\tilde{z}_{|3}||_{(H^\sigma([0,T];L^2(\Omega)))^*} &\leq ||\tilde{z}||_{(H^\sigma([0,T];H^1_{0,\Gamma}(\Omega)^*))^*} \quad \text{and} \\
||(\mathbf{B}\tilde{v})_3||_{(H^\sigma([0,T];L^2(\Omega)))^*} &\leq ||\tilde{v}||_{(H^\sigma([0,T];H^1_{\mathbf{B}}(\Omega)^*))^*}. \qquad (3.13)
\end{aligned}
$$

The values in (3.13) are, by our assumption on the solution operator of the adjoint equation, bounded by some constant times $||z||_{(H^\sigma([0,T]))^*}$. The terms in (3.12) with norms in $H^\sigma([0,T], L^2(\Omega))$ including the function $e^{-i\phi_{|3}\omega}$ can be estimated with the help of the following interpolation inequality

$$
\forall v \in H^2[0,T]\ :\quad ||v||_{H^\sigma[0,T]} \leq ||v||^{2-\sigma}_{H^1[0,T]} ||v||^{\sigma-1}_{H^2[0,T]}, \qquad (3.14)
$$

which is a Nirenberg-Gagliardo type interpolation inequality [3, 17]. Now, the first and second time derivatives of $e^{-i\phi_{|3}\omega}\phi_{|3}$ are

$$
\begin{aligned}
\frac{d}{dt} e^{-i\phi_{|3}\omega} \phi_{|3} &= e^{-i\phi_{|3}\omega} \left(-i\phi^2_{|3}\omega \frac{d}{dt}\phi_{|3} + \frac{d}{dt}\phi_{|3} \right) \\
\frac{d^2}{dt^2} e^{-i\omega\phi_{|3}} \phi_{|3} &= e^{-i\phi_{|3}\omega} \left(-\omega^2 \phi^3_{|3} \left(\frac{d}{dt}\phi_{|3} \right)^2 - 3i\phi_{|3}\omega (\frac{d}{dt}\phi_{|3})^2 \right) \\
&\quad + e^{-i\phi_{|3}\omega} \left(-i\phi_{|3}\omega \frac{d^2}{dt^2}\phi_{|3} + \frac{d^2}{dt^2}\phi_{|3} \right). \qquad (3.15)
\end{aligned}
$$

Thus with $\mathbf{u}$ and $\phi \in C^\infty$

$$\begin{aligned}
&\left(\frac{1}{1+\omega^2}\right)^2 ||e^{-i\omega\phi_{|3}}\phi_{|3}||_{(H^\sigma[0,T];L^2(\Omega))} \\
&= \mathcal{O}\left(\left(\frac{1}{1+\omega^2}\right)^2\right)\mathcal{O}\left((\omega^{(2-\sigma)})^2\right)\mathcal{O}\left(((\omega^2)^{\sigma-1})^2\right) \\
&= \mathcal{O}\left(\left(\frac{1}{1+\omega^2}\right)^2\right)\mathcal{O}\left(\left(\frac{1}{1+\omega^2}\right)^{-2+\sigma}\right)\mathcal{O}\left(\left(\frac{1}{1+\omega^2}\right)^{2-2\sigma}\right) \\
&= \mathcal{O}\left(\frac{1}{1+\omega^2}\right)^{2-\sigma}. \qquad (3.16)
\end{aligned}$$

We can argue analogously for $||e^{-i\omega\phi_{|3}}(\mathbf{Bu})_3||_{(H^\sigma[0,T];L^2(\Omega))}$. Finally this gives together with (3.12)

$$||F'(e_{33},\varepsilon_{33}^S)^*[z]||_{(H^2(\mathbb{R}))^2} \leq C||z||_{(H^\sigma[0,T])^*}\int_{\mathbb{R}}\left(\frac{1}{1+\omega^2}\right)^{2-\sigma}d\omega.$$

The integral here over $\mathbb{R}$ remains finite as long as $\sigma < 3/2$. Since $L^2[0,T]$ is dense in $(H^\sigma[0,T])$ it follows that $F'(e_{33},\varepsilon_{33}^S)^*$ can be extended to a continuous linear operator mapping from $(H^\sigma[0,T])^*$ to $(H^2(\mathbb{R}))^2$ for any $\sigma \in (0,3/2)$. □

This allows for the interpretation of the adjoint operator being smoothing of order $\frac{3}{2}$. As it is similarly shown in [7]

$$\begin{aligned}
&||F'(e_{33},\varepsilon_{33}^S)[s]||_{H^\sigma[0,T]} \\
&\qquad = \sup_{z\in Y}\frac{(F'(e_{33},\varepsilon_{33}^S)[s],z)_{L^2[0,T]}}{||z||_{(H^\sigma[0,T])^*}} \\
&\qquad = \sup_{z\in Y}\frac{(s,F'(e_{33},\varepsilon_{33}^S)^*[z])_{(H^2(\mathbb{R}))^2}}{||z||_{(H^\sigma[0,T])^*}} \\
&\qquad \leq ||F'(e_{33},\varepsilon_{33}^S)^*||_{(H^\sigma[0,T])^*\to(H^2(\mathbb{R})^2}||s||_{(H^2(\mathbb{R}))^2}
\end{aligned}$$

for any $s \in X$ and $\sigma \in (0,3/2)$. Hence, the range $\mathcal{R}(F'(e_{33},\varepsilon_{33}^S))$ of the linearization of the forward operator F is nonclosed in Y which shows even the ill-posedness of the linearized problem.

3.2. Numerical Results

In this section numerical identification results using synthetically generated data will be presented. The main intention of this section is to test the iterative multilevel algorithm, described in detail in Algorithm 2.1. The discretization of the parameter curves is implemented with cubic splines. The refinement of discretization when going from

level N to level $N+1$ is done by bisection of each subinterval. The coarsest level always consists of three grid points only. For the implementation of the inner stopping rule a term including information about the size of the discretization intervals, the data error and appropriate scaling factors is evaluated according to

$$||F(e_{33}^k, \varepsilon_{33}^{S,k}) - y^\delta|| \leq C_1(c_1\delta + c_2\frac{1}{2^N}). \tag{3.17}$$

The discretization error may be estimated by $\inf_{S\in\mathbb{S}_h^k} ||f-S||_{H^j(\Omega)} \leq ch^{k-j}||f||_{H^k(\Omega)}$ for any spline S of order k with uniform knots and width h [24].

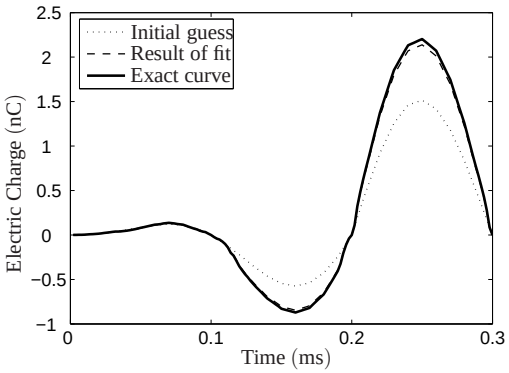

Figure 3: Charge response with constant (initial guess, dotted) and nonlinear permittivity (exact and fitted data, solid and dashed).

In a first step we report on reconstructing just the permittivity as a function of the electric field. As initial guess we use a constant function with the value obtained in the small signal case, see Figures 5-6. As excitation a special signal with zero charge and zero derivative for $t = 0$ is chosen. The electric charge serves as measurements, see Figure 3

Figure 4 shows the development of the residual during the multilevel algorithm for different choices of the damping parameter ω_N^k. Along the abscissa the accumulated inner iteration index is plotted, vertical lines show a transition between two levels. The horizontal line shows the quantity $C_2\delta$. As we see, both the steepest descent and minimal error variant behave rather similarly and proceed (by coincidence) to the next finer level after the same amount of inner iterations. Two different types of functions have been reconstructed, see Figures 5-6, which are assumed to be physically reasonable. Results of the simultaneous reconstruction of the two parameter curves e_{33} and ε_{33}^S are given in Figure 8. The reconstruction seems to be robust with respect to errors in the data. However, in particular for lower field intensities one sees less satisfying reconstruction results which might be due to the fact that the material parameters mutually influence each other.

Concerning computation times the following can be observed: During the multilevel algorithm the computation of the discretized adjoint problem is performed before the

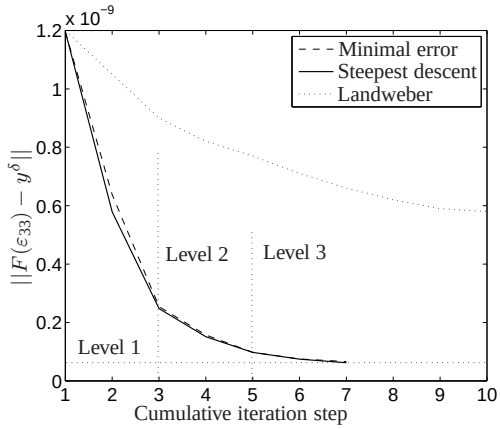

Figure 4: Development of residual norm for different choices of ω during reconstruction of the permittivity (for the curve in Figure 6) with one percent data noise.

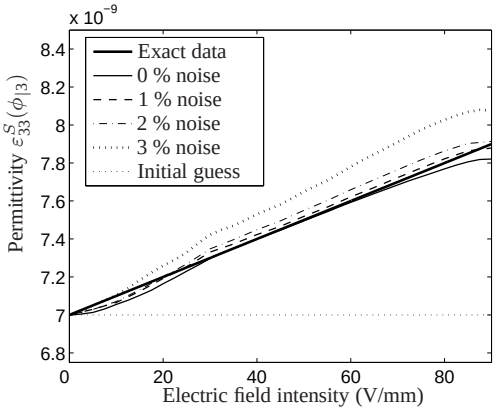

Figure 5: Reconstruction of a linear parameter curve with different amounts of data noise.

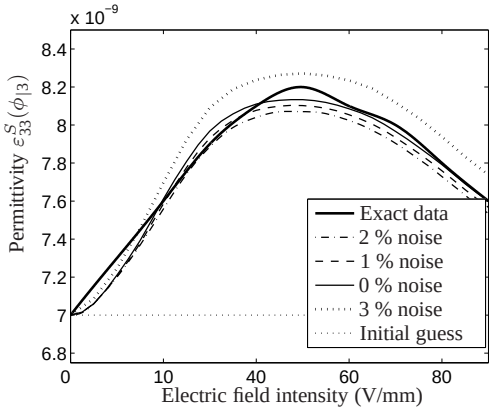

Figure 6: Reconstruction of a parabolic parameter curve with different amounts of data noise.

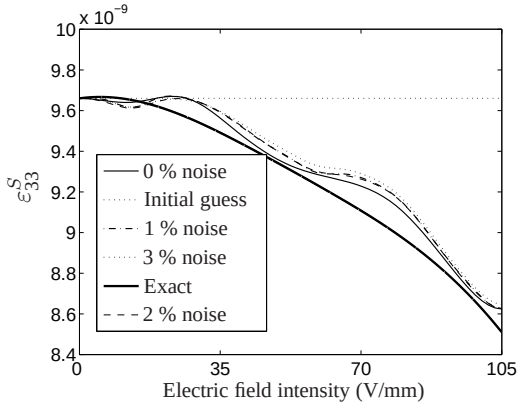

Figure 7: Simultaneously reconstructed parameter curves, here $\varepsilon_{33}^S(\phi_{|3})$, with different amounts of data noise.

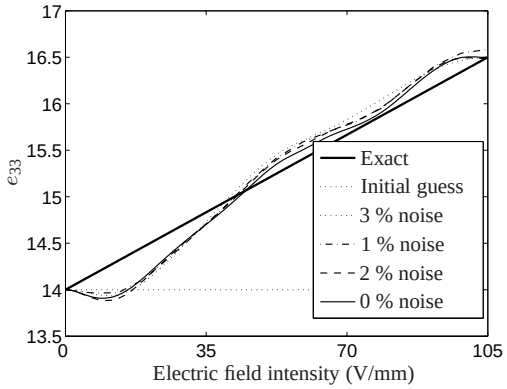

Figure 8: Simultaneously reconstructed parameter curves, here $\mathbf{e}_{33}(\phi_{|3})$, with different amounts of data noise.

projection of the solution onto the current level. So the computing time on each level for the adjoint problem is nearly the same. And since it is a linear problem, the solution is distinctly less expensive than that for a single forward solve which is a nonlinear PDE. Nevertheless, the multilevel strategy pays off concerning computing times since information at different levels are taken into account which decreases remarkably the over-all number of modified Landweber iterations compared to a strategy where one immediately starts on some fine and fixed level. Table 1 tries to quantify the observations. The values listed stem from the reconstruction of the curve in Figure 6 with one per cent data noise. Here, first we counted the number of minimal error iterations and the CPU time on each level, where the iterative multilevel algorithm passed five different levels to reach a prescribed residual of 0.1e-09. Then we restarted the algorithm on that level (level 4), which guarantees the same resolution of the sought-for quantities, hold the number of nodes fixed, and counted the required number of iterations and CPU-time, see last row in Table 1.

Level	Number of Nodes	Number of Iterations	CPU time	Residual
0	3	1	37.0s	1.6e-09
1	5	1	38.3s	0.31e-09
2	9	4	153.1s	0.28e-09
3	17	3	112.2s	0.12e-09
4	33	2	81.9s	0.102e-09
fixed level:	33	28	1090.0 s	0.101e-09

Table 1. Number of iterations and computing times on different levels.

3.3. Conclusions and Outlook

The proposed iterative multilevel algorithm can be applied to any arbitrary identification or more general to any nonlinear inverse problem where discretizations of the sought-for quantity are involved. Regarding just the numerics the choice of the modified Landweber iterations has turned out to be be a powerful algorithm due to an optimal steering of the step-length parameter. Of course, the inner iterations might be substituted by any other regularizing iterative method, e.g. inexact Newton methods or others discussed e.g. in [9].

The application, parameter curve identification in nonlinear piezoelectricity, is rather problem oriented. Here, an open task is the identification from real world measurements. It is open yet, if the functional dependencies can be reduced to one or two unknowns as it is done in this work and how appropriate measurements need to be conducted in order to mask interactions with other tensor entries.

Acknowledgments. In particular I would like to thank Prof. Dr. B. Kaltenbacher for her valuable comments during the development of this paper which tackles parts of the topics of my PhD-Thesis. As mentioned, the work at hand is supported by the German Science Foundation DFG under grant Ka 1778/1.

References

1. W. G. Cady, 1, *Piezoelectricity - An Introduction to the Theory and Applications of Electromechanical Phenomena in Crystals*. Dover Publications, INC, 1964.
2. H. W. Engl, M. Hanke, and A. Neubauer, *Regularization of Inverse Problems*. Kluwer, Dordrecht, 1996.
3. E. Gagliardo, Ulteriori proprieta di alcune classi di funzioni in piu variable. *Ricerche di Mat.* **8** (1959), 24–51.
4. G. H. Gautschi, *Piezoelectric Sensorics*. Springer-Verlag, Berlin, Heidelberg, New York, 2006.
5. C. Gerthsen, 21, *Gerthsen Physik*. Springer - Verlag Berlin, Heidelberg, New York, 2002.
6. *IEEE Standard on Piezoelectricity*, 1985, IEEE/ANSI.
7. B. Kaltenbacher, M. Kaltenbacher, and Reitzinger S., Identification of nonlinear B-H curves based on magnetic field computations and multigrid methods for ill-posed problems. *European Journal of Applied Mathematics* **14** (2003), 15–38. DOI: 10.1017/S0956792502005089.
8. B. Kaltenbacher, T. Lahmer, and M. Mohr, PDE based determination of piezoelectric material tensors. *European Journal of Applied Mathematics* **17** (2006), 383–416. DOI: 10.1017/S0956792506006474.
9. B. Kaltenbacher, A. Neubauer, and O. Scherzer, *Iterative Regularization Methods for Nonlinear Ill-Posed Problems*, To appear.
10. M. Kaltenbacher, *Numerical Simulation of Mechatronic Sensors and Actuators*. Springer Verlag Berlin-Heidelberg, 2004.
11. M. Kamlah, Ferroelectric and ferroelastic piezoceramics - modeling of electromechanical hysteresis phenomena. *Continuum Mechanics and Thermodynamics, Springer Berlin / Heidelberg* **13** (2001), 219–268.
12. E. Kittinger, E. Tichy, and W. Friedel, Nonlinear piezoelectricity and electrostriction of alpha quartz. *Journal of Applied Physics* **60** (1986), 1465–1471.
13. K. Kunisch and G. Geymayer, *Convergence rates for regularized nonlinear illposed problems*, 154, Book Series Lecture Notes in Control and Information Sciences, Springer Berlin / Heidelberg, 1991, DOI: 10.1007/BFb0044485, 81–92.
14. T. Lahmer, *Direct and Inverse Problems in Piezoelectricity*, Ph.D. thesis, Friedrich-Alexander University, Erlangen-Nuremberg, Germany, 2008.
15. A. Neubauer and O. Scherzer, Finite-dimensional approximation of tikhonov regularized solutions of non-linear ill-posed problems. *Numerical Functional Analysis and Optimization* **11** (1990).
16. _____, A convergence Rate Result for a Steepest Descent Method and a Minimal Error method for the Solution of Nonlinear Ill-Posed Problems. *Z. Anal. Anwend.* **14** (1995), 369–377.
17. L. Nirenberg, An extended interpolation inequality. *Annali della Scuola Normale Superiore di Pisa - Classe di Scienze Sér 3* **20** (1966).

18. M. K. Samal, P. Seshu, S. Parashar, U. von Wagner, P. Hagedorn, and B. K. Dutta, A finite element model for nonlinear behavior of piezoceramics under weak electric fields. *Finite Elements in Analysis and Design* **41** (2005), 1464–1480.

19. M. K. Samal, P. Seshu, S. Parashar, U. von Wagner, P. Hagedorn, B. K. Dutta, and H.S. Kushwaha, Nonlinear behaviour of piezoceramics under weak electric fields. Part II: Numerical results and validation with experiments. *International Journal of Solids and Structures* **43** (2006), 1437–1458.

20. O. Scherzer, A Convergence Analysis of a Method of Steepest Descent And a Two-Step Algorithm for Nonlinear Ill-Posed Problems. *Numer. Funct. Anal. and Optimiz.* (1996), 197–214.

21. _____, An iterative multi level algorithm for solving nonlinear ill-posed problems. *Numer. Math.* (1998), :579–600.

22. O. Scherzer and T. Strohmer, A multi-level algorithm for the solution of moment problems. *Numerical Functional Analysis and Optimization* **19** (1998), 353 – 375.

23. R. C. Smith, *Smart material systems, model development*, Frontiers in applied mathematics. SIAM, 2005.

24. Yu.N. Subbotin, Extremal functional interpolation and approximation by splines. *Mat. Zametki* **15** (1974), 843–854.

Received 12 April, 2007; revised 13 July, 2007

Author information

Tom Lahmer, Paul-Gordan Str. 3-5, 91052 Erlangen, Germany.
Email: tom.lahmer@lse.eei.uni-erlangen.de